

Transmission Line Fault Detection Using Synchrophasor

Miss. Bharti R Phirke¹, Prof. D. S. Chavan²

^{1,2}Electrical Engineering Bharati Vidyapeeth Deemed University College of Engineering Pune, India

Abstract: The accuracy in fault detection and location is always a challenge for a power system engineer. The current differential protection has the highest reliability among all types of protection scheme, but it is not being used for transmission line protection because of certain problems such as CT ratio mismatch, pilot wire length, tap changing transformer etc. This paper describes the details about the synchrophasor technology which uses the GPS based time synchronization having the accuracy of the order of $1\mu\text{s}$. This paper explored the flexibility of the synchrophasor technology based current differential protection in Matlabsimulink and presented the results for all types of faults with different fault resistance, inception angle, and fault location, and it is observed the current differential protection using synchrophasor technology has almost the 100% reliability.

Keywords: current differential protection, charging current compensation, synchrophasor.

I. Introduction

Most of limitations of current differential protection can be overcome by digital current differential protection based on microcomputer by using digital communication link. For digital differential protection, to make differential comparison, not the current waveforms varying with time, to satisfy the requirement of current differential principle. The sample of protected line from all terminals can be time aligned in synchronization. This kind of protection can be implemented using this technique, is known as synchronization Technology and GPS are given. This is completely new technology. By using this technology for current differential protection for transmission line having ideally no limit fits length.

II. New Theory Of Current Differential Protection

Capacitive current [1] could be using several new theories. Several ways to overcome capacitive current have been suggested. Current differential protection will be able to overcome the capacitive current as a way to protect UHV transmission line system. But these new theories have to be tested and implemented as in electric power system. The relay protection reliability requirements are strict and precise. Therefore a simple and feasible way to improve current differential protection which can compensate steady capacitive current and transient without increasing the computation consumption, sampling rate, computation consumption and telecommunication channel. Time domain compensation algorithm [2], for performing the differential equation for transmission line of π equivalent circuit has been implemented recently. This algorithm is supposed to solve the capacitive current problem for steady and transient distributed capacitive current.

III. Differential Protection Scheme For Transmission Line Using Synchrophasors

3.1 The System to Be Simulated

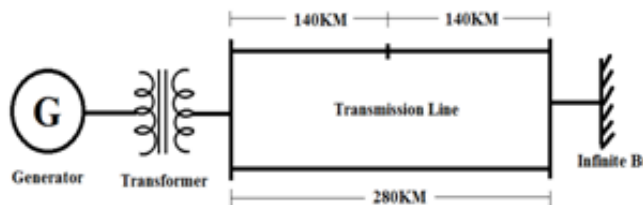


Fig. 1. Simulated System Single Line Diagram

Specifications

Generator- 600MVA, 22KV, 60Hz, H= 4.4MW-S/MVA,
 $X_d = 1.81\text{pu}$, $X_d' = 0.3\text{pu}$, $X_d'' = 0.23\text{pu}$,
 $T_{d0}' = 8\text{s}$, $T_{d0}'' = 0.03\text{s}$, $X_q = 1.76\text{pu}$,
 $X_q' = 0.25\text{pu}$, $T_{q0}'' = 0.03\text{pu}$,

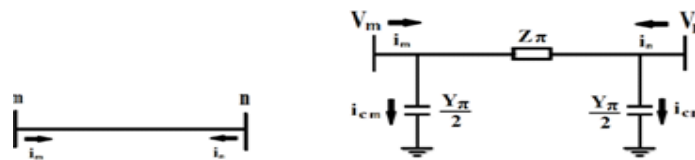
Ra=0.003pu, Xp=0.15pu.
 Transformer- 600MVA, 22/400KV, 60Hz,
 Delta-Star, X=0.163pu, Xcore=0.33pu,
 Rcore=0, Pcopper= 0.00177pu
 Transmission Lines- Z1=0.12+j0.88 ohm/km,
 Z0=0.309 +j1.297ohm/km, C1=1.0876*10⁻⁰⁸ F/KM

The system is simulated using MATLAB 7.8 software. Here we have consider the power factor of 0.9 lagging, therefore the active power transfer from sending end generator is 540MW, also for load flow analysis we have considered the PV bus with voltage of 22KV.

3.2 Times-Domain Algorithm for Capacitive Current Compensation

3.2.1 Transmission Line Model

Fig 2 Shows The Transmission Line Π-Circuit And Its Equivalent Connection.



a) Equivalent connection b) π equivalent circuit

Fig.2 Equivalent connection and circuit of transmission line.

The distributed phase parameters are supposed to be uniform, symmetrical and positive current direction flows toward line from bus for both terminals as an analysis for a long distance UHV transmission line of protective relay behavior. Expression for equivalent parameter of transmission line is given below.

$$Z = Z_c \sin \gamma l \tag{1}$$

$$Y = \frac{2(\cosh \gamma l - 1)}{Z_c \sin \gamma l} \tag{2}$$

Where Z & Y are the equivalent impedance and the equivalent admittance, $Z_c = \sqrt{Z/Y}$ the surge impedance, $\gamma = \sqrt{zy}$ the propagation coefficient, l is length of line, z and y the impedance and admittance per-unit length of the line respectively.

The actual three-phase power system is separated to α, β, o modal components system by using Karenbauer phase-mode transformation for transient state analysis caused by unsymmetrical faults in time-domain. Each module network is satisfy equation (1), (2) i.e equivalent parameters of a modal network are describe below

$$Z\pi\alpha = Zc\alpha \sin \gamma\alpha l \tag{3}$$

$$Y\pi\alpha = \frac{2(\cosh \gamma\alpha l - 1)}{Zc\alpha \sin \gamma\alpha l} \tag{4}$$

where $Z\pi\alpha$ is α modal surge impedance, $Y\pi\alpha$ is α modal equivalent admittance, $Zc\alpha = \sqrt{Z\alpha/Y\alpha}$ is α modal surge impedance, $\gamma\alpha = \sqrt{Z\alpha Y\alpha}$ is α modal propagation coefficient, l line length, $Z\alpha$ and $Y\alpha$ α modal impedance and admittance per-unit length of the line, respectively. Modal networks for β and o can also be obtained same as above equation. Above certain higher order harmonics frequency there are many distinguishing frequency characteristics between distributed parameter and π model network. Below this frequency there are similar characteristics for both model network. They are similar under fundamental frequency condition. The applicable frequency range is not fixed but depends on system impedance and length of line for each model based as per some simulations. The applicable frequency range are 0-200Hz and 0-800Hz are the frequency ranges for R-L and π respectively for short line. They drop to 0-100Hz and 0-200Hz respectively for long lines, whereas for entire frequency range, the distributed parameter model is applicable.

The π model can be behaved as time domain model by filtering out the high order harmonics that are higher than a certain frequency. Fig 3 shows the π equivalent circuit of a model network in time domain (sample

based). Where C_α , R_α and L_α are a modal equivalent capacitance of the line, modal equivalent resistance and inductance of the transmission line, respectively. The β and o modal networks have similar equivalent circuits.

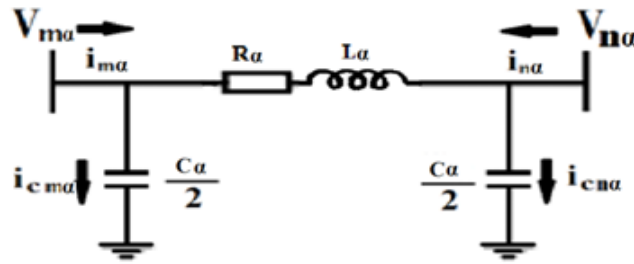


Fig.3 Equivalent circuit of α modal network in time domain

3.2.2 Calculation of Capacitive Current Compensation

The time domain compensation calculation process is explained, using fig.3 α modal network. First, transform the sampled data into modal quantities. The phase-to- modal transformation and its inverse are given below.

$$\begin{bmatrix} I_o \\ I_\alpha \\ I_\beta \end{bmatrix} = \frac{1}{3} \begin{bmatrix} 1 & 1 & 1 \\ 1 & -1 & 0 \\ 1 & 0 & -1 \end{bmatrix} \begin{bmatrix} I_a \\ I_b \\ I_c \end{bmatrix} \tag{5}$$

$$\begin{bmatrix} I_a \\ I_b \\ I_c \end{bmatrix} = \frac{1}{3} \begin{bmatrix} 1 & 1 & 1 \\ 1 & -2 & 1 \\ 1 & 1 & -2 \end{bmatrix} \begin{bmatrix} I_o \\ I_\alpha \\ I_\beta \end{bmatrix} \tag{6}$$

Values for modal instantaneous values of the capacitive currents to be compensated at terminals m and n can be calculated as follows.

$$I_{c m \alpha}(t) = \frac{C_\alpha}{2} \frac{d(V_{m \alpha}(t))}{dt} \tag{7}$$

$$I_{c n \alpha}(t) = \frac{C_\alpha}{2} \frac{d(V_{n \alpha}(t))}{dt} \tag{8}$$

A modal instantaneous values of the voltage on the buses at both m and m terminals are $V_m \alpha(t)$ and $V_n \alpha(t)$ respectively.

For half-length, modal instantaneous line currents compensated in time domain at terminal m and n, using KCL is as below

$$I_{m \alpha}(t)' = I_{m \alpha}(t) - \frac{C_\alpha}{2} \frac{d(V_{m \alpha}(t))}{dt} \tag{9}$$

$$I_{n \alpha}(t)' = I_{n \alpha}(t) - \frac{C_\alpha}{2} \frac{d(V_{n \alpha}(t))}{dt} \tag{10}$$

where $I_{m \alpha}(t)$ and $I_{n \alpha}(t)$ are the pre-compensation instantaneous values and $I_{m \alpha}(t)'$, $I_{n \alpha}(t)'$ are the post-compensation instantaneous values of α modal line currents at terminals m and n, respectively. Same process can be followed for instantaneous values calculation of β and o modal line currents after half-length compensation. Substitute α , β and o modal instantaneous line currents to equation (6) of inverse phase-mode transformation

$$\begin{bmatrix} I_{m a} \\ I_{m b} \\ I_{m c} \end{bmatrix} = \frac{1}{3} \begin{bmatrix} 1 & 1 & 1 \\ 1 & -2 & 1 \\ 1 & 1 & -2 \end{bmatrix} \begin{bmatrix} I_{m o}' \\ I_{m \alpha}' \\ I_{m \beta}' \end{bmatrix} \tag{11}$$

$$\begin{bmatrix} I_{n a} \\ I_{n b} \\ I_{n c} \end{bmatrix} = \frac{1}{3} \begin{bmatrix} 1 & 1 & 1 \\ 1 & -2 & 1 \\ 1 & 1 & -2 \end{bmatrix} \begin{bmatrix} I_{n o}' \\ I_{n \alpha}' \\ I_{n \beta}' \end{bmatrix} \tag{12}$$

Where $I_{m a}$, $I_{m b}$, $I_{m c}$, $I_{n a}$, $I_{n b}$ and $I_{n c}$ are the three phase instantaneous currents for time domain half length compensation calculated at both ends of the transmission line.

3.2.3 Simulation Diagrams for Time Domain Compensation

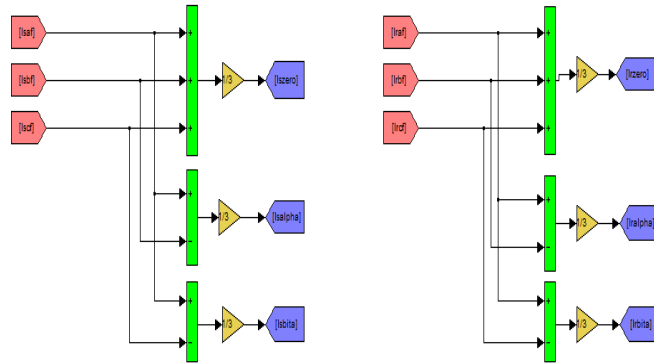


Fig. 4 Calculation of o , α and β components of sending and receiving end current

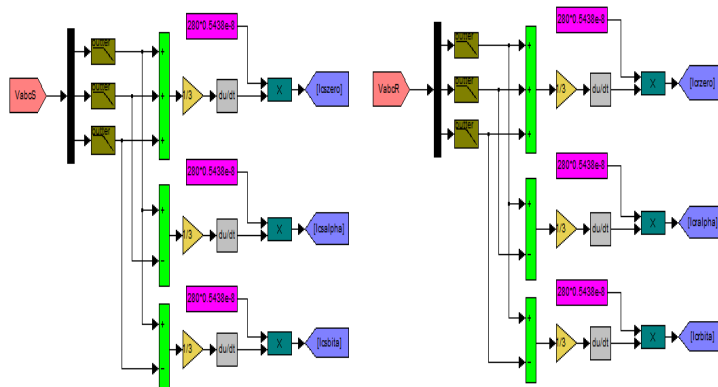


Fig. 5 Calculation of charging current components of sending and receiving end.

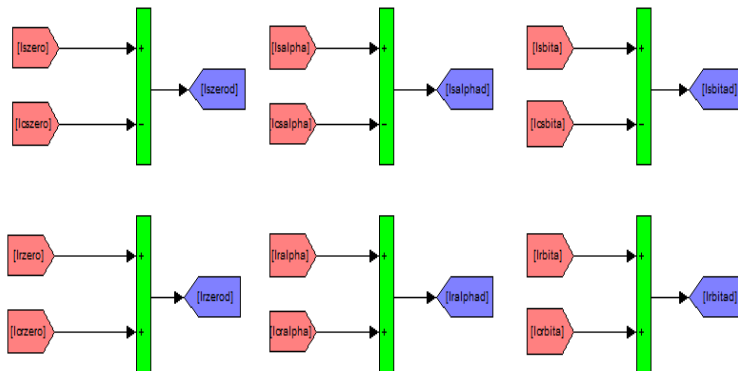


Fig.6 Calculation of I_{m0} , $I_{m\alpha}$, $I_{m\beta}$ and I_{n0} , $I_{n\alpha}$, $I_{n\beta}$ currents.

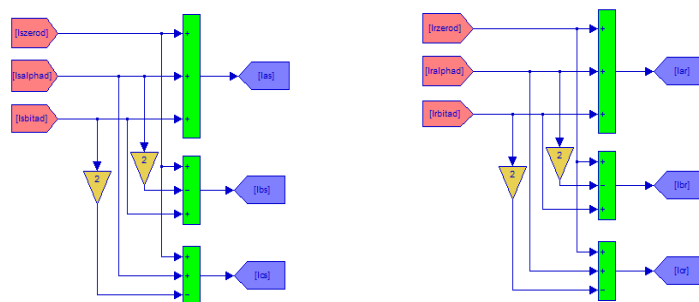


Fig.7 Calculation of sending and receiving end line currents after compensation

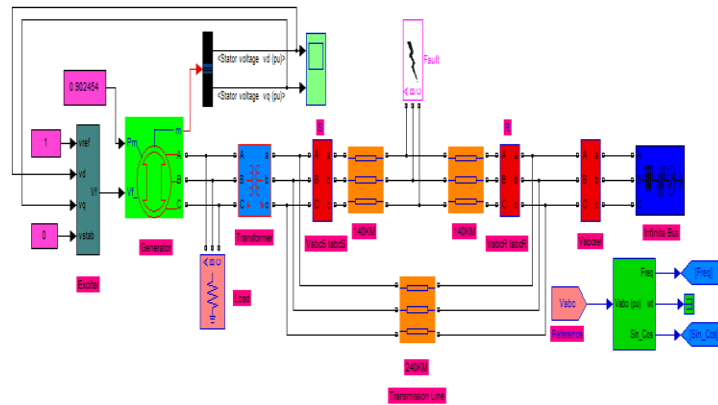


Fig. 8 Power system simulated for testing current differential protection for internal and external faults with time domain compensation for charging current.

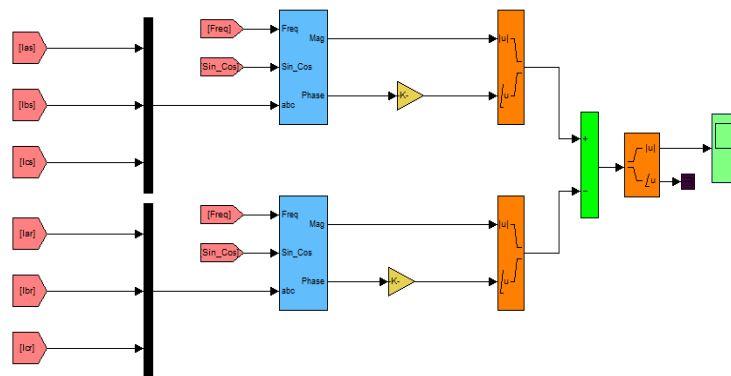


Fig. 9.Simulation diagram for finding difference of sending end and receiving end positive sequence current.

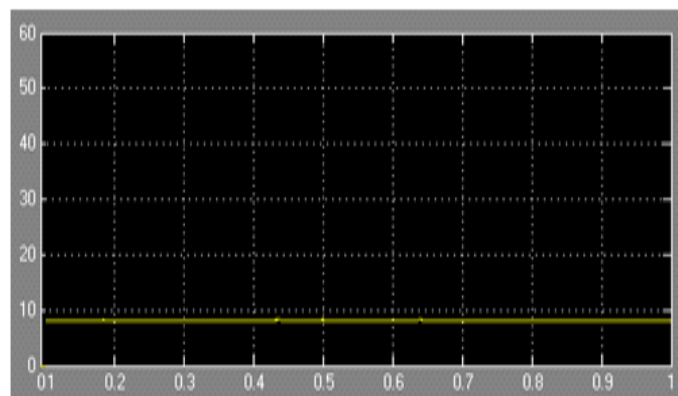


Fig 10.Difference of sending end and receiving end positive sequence current without any fault.

As described earlier, WAP and M based transmission line protection makes use of Differential protection scheme which is simulated in the shown system. With transmission line, generator and infinite bus parameters kept same.

The fault analysis is done by varying:

1. Type of fault:
 - a) L-G b) L-L c) L-L-G d) L-L-L-G (3phase balanced Fault)
2. Location 10%, 50% 90% (for 280 Km line)
3. Fault resistance
 - a) Very small (0.001Ω) b) Medium (10Ω) c) High (100Ω)

These sending-end and receiving-end current waveforms are then sent to PMU for phasor measurement, where by using additional modules in existing system we compute positive sequence component of both sending-end and receiving-end currents.

These respective components of sending-end and receiving-end currents are then compared as if it is a ‘current differential’ protection scheme. Deploy a protection scheme on the fact that as the differential sequence currents exceed certain set values of sequence currents the Differential distance protection scheme will issue a trip command. By the works of Fortescue’s, an unbalanced system of n related phasors is equivalent to n systems of balanced phasors. These are called the symmetric components of the original phasors.

For each set of component, n phasors are equal in length and angle is set equal between phasors adjacent to each other.

Three phase unbalanced system three balanced systems of phasors

1. Positive sequence component which include same magnitude of 3 phasors which are separated by 120° from each other and having same phase sequence as the original phasors.
2. Negative sequence component which include same magnitude of 3 phasors which are separated by 120° from each other. This phase sequence and sequence of original phasors are opposite to each other .
3. Zero sequence components which include same magnitude of 3 phasors and with zero phase displacement from each other.

- $I_a = I_{a1} + I_{a2} + I_{a0}$
- $I_b = I_{b1} + I_{b2} + I_{b0}$
- $I_c = I_{c1} + I_{c2} + I_{c0}$

Traditionally these components can be obtained by using the operator viz. α

$$\alpha = 1 \angle 120^\circ = -0.5 + j0.866$$

- $I_{b1} = \alpha^2 I_{a1}$ $I_{c1} = \alpha I_{a1}$
- $I_{b2} = \alpha I_{a2}$ $I_{c2} = \alpha^2 I_{a2}$
- $I_{b0} = I_{a0}$ $I_{c0} = I_{a0}$

3.2.4 Fault Analysis

Table 1. Shows the results of fault analysis for L-G fault at different fault resistance, different fault location, and different fault inception angle.

Table 1. L-G Fault Analysis

SR NO	Type of Fault	Inception angle(α)	Fault Location	Fault Resistance(Rf)	Differential Current (Id)
1	L-G	0°	14KM	0.001Ω	1460A
2	L-G	0°	14KM	10Ω	1446A
3	L-G	0°	14KM	100Ω	844A
4	L-G	0°	140KM	0.001Ω	1130A
5	L-G	0°	140KM	10Ω	1106A
6	L-G	0°	140KM	100Ω	716A
7	L-G	0°	266KM	0.001Ω	6350A
8	L-G	0°	266KM	10Ω	4937A
9	L-G	0°	266KM	100Ω	935A
10	L-G	45°	14KM	0.001Ω	1463A
11	L-G	45°	14KM	10Ω	1448A
12	L-G	45°	14KM	100Ω	845A
13	L-G	45°	140KM	0.001Ω	1135A
14	L-G	45°	140KM	10Ω	1108A
15	L-G	45°	140KM	100Ω	717A
16	L-G	45°	266KM	0.001Ω	6355A
17	L-G	45°	266KM	10Ω	4938A
18	L-G	45°	266KM	100Ω	936A
19	L-G	90°	14KM	0.001Ω	1467A
20	L-G	90°	14KM	10Ω	1449A
21	L-G	90°	14KM	100Ω	845A
22	L-G	90°	140KM	0.001Ω	1137A
23	L-G	90°	140KM	10Ω	1107A
24	L-G	90°	140KM	100Ω	718A
25	L-G	90°	266KM	0.001Ω	6358A
26	L-G	90°	266KM	10Ω	4941A
27	L-G	90°	266KM	100Ω	936A

Table 2 shows the results of fault analysis for L-L fault at different fault resistance, different fault location, and different fault inception angle.

Table 2. L-L Fault Analysis

SR NO	Type of Fault	Inception angle(α)	Fault Location	Fault Resistance(Rf)	Differential Current (Id)
1	L-L	0°	14KM	0.001Ω	1920A
2	L-L	0°	14KM	10Ω	1900A
3	L-L	0°	14KM	100Ω	1226A
4	L-L	0°	140KM	0.001Ω	1815A
5	L-L	0°	140KM	10Ω	1784A
6	L-L	0°	140KM	100Ω	1134A
7	L-L	0°	266KM	0.001Ω	10880A
8	L-L	0°	266KM	10Ω	8200A
9	L-L	0°	266KM	100Ω	1418A
10	L-L	45°	14KM	0.001Ω	1922A
11	L-L	45°	14KM	10Ω	1901A
12	L-L	45°	14KM	100Ω	1227A
13	L-L	45°	140KM	0.001Ω	1816A
14	L-L	45°	140KM	10Ω	1787A
15	L-L	45°	140KM	100Ω	1136A
16	L-L	45°	266KM	0.001Ω	10883A
17	L-L	45°	266KM	10Ω	8202A
18	L-L	45°	266KM	100Ω	1420A
19	L-L	90°	14KM	0.001Ω	1925A
20	L-L	90°	14KM	10Ω	1904A
21	L-L	90°	14KM	100Ω	1229A
22	L-L	90°	140KM	0.001Ω	1818A
23	L-L	90°	140KM	10Ω	1789A
24	L-L	90°	140KM	100Ω	1137A
25	L-L	90°	266KM	0.001Ω	10887A
26	L-L	90°	266KM	10Ω	8206A
27	L-L	90°	266KM	100Ω	1422A

Table .3.shows the results of fault analysis for L-L-G fault at different fault resistance, different fault location, and different fault inception angle.

Table.3. L-L-G Fault Analysis

SR NO	TypeOf fault	Inception angle(α)	Fault Location	Fault Resistance (Rf)	Differential Current (Id)
1	L-L-G	0°	14KM	0.001Ω	2500A
2	L-L-G	0°	14KM	10Ω	2490A
3	L-L-G	0°	14KM	100Ω	1655A
4	L-L-G	0°	140KM	0.001Ω	2280A
5	L-L-G	0°	140KM	10Ω	2240A
6	L-L-G	0°	140KM	100Ω	1468A
7	L-L-G	0°	266KM	0.001Ω	13660A
8	L-L-G	0°	266KM	10Ω	10435A
9	L-L-G	0°	266KM	100Ω	1880A
10	L-L-G	45°	14KM	0.001Ω	2502A
11	L-L-G	45°	14KM	10Ω	2493A
12	L-L-G	45°	14KM	100Ω	1656A
13	L-L-G	45°	140KM	0.001Ω	2282A
14	L-L-G	45°	140KM	10Ω	2242A
15	L-L-G	45°	140KM	100Ω	1469A
16	L-L-G	45°	266KM	0.001Ω	13663A
17	L-L-G	45°	266KM	10Ω	10436A
18	L-L-G	45°	266KM	100Ω	1881A
19	L-L-G	90°	14KM	0.001Ω	2505A
20	L-L-G	90°	14KM	10Ω	2493A
21	L-L-G	90°	14KM	100Ω	1657A
22	L-L-G	90°	140KM	0.001Ω	2285A
23	L-L-G	90°	140KM	10Ω	2245A
24	L-L-G	90°	140KM	100Ω	1472A
25	L-L-G	90°	266KM	0.001Ω	13666A
26	L-L-G	90°	266KM	10Ω	10437A
27	L-L-G	90°	266KM	100Ω	1884A

Table .4.shows the results of fault analysis for L-L-L-G fault at different fault resistance, different fault location, and different fault inception angle.

Table .4. L-L-L-G Fault Analysis

SR NO	Type of Fault	Inception angle(α)	Fault Location	Fault Resistance(Rf)	Differential Current (Id)
1	L-L-L-G	0°	14KM	0.001Ω	3350A

2	L-L-L-G	0°	14KM	100Ω	3300A
3	L-L-L-G	0°	14KM	100Ω	2420A
4	L-L-L-G	0°	140KM	0.001Ω	3400A
5	L-L-L-G	0°	140KM	10Ω	3360A
6	L-L-L-G	0°	140KM	100Ω	2240A
7	L-L-L-G	0°	266KM	0.001Ω	21400A
8	L-L-L-G	0°	266KM	10Ω	16350A
9	L-L-L-G	0°	266KM	100Ω	2838A
10	L-L-L-G	45°	14KM	0.001Ω	3352A
11	L-L-L-G	45°	14KM	10Ω	3302A
12	L-L-L-G	45°	14KM	100Ω	2423A
13	L-L-L-G	45°	140KM	0.001Ω	3403A
14	L-L-L-G	45°	140KM	10Ω	3361A
15	L-L-L-G	45°	140KM	100Ω	2242A
16	L-L-L-G	45°	266KM	0.001Ω	21403A
17	L-L-L-G	45°	266KM	10Ω	16353A
18	L-L-L-G	45°	266KM	100Ω	2840A
19	L-L-L-G	90°	14KM	0.001Ω	3355A
20	L-L-L-G	90°	14KM	10Ω	3304A
21	L-L-L-G	90°	14KM	100Ω	2426A
22	L-L-L-G	90°	140KM	0.001Ω	3405A
23	L-L-L-G	90°	140KM	10Ω	3366A
24	L-L-L-G	90°	140KM	100Ω	2245A
25	L-L-L-G	90°	266KM	0.001Ω	21408A
26	L-L-L-G	90°	266KM	10Ω	16357A
27	L-L-L-G	90°	266KM	100Ω	2844A

Fig. 11 shows the minimum differential fault current from the above fault analysis tables for the condition L-G Fault, 0° inception angle, fault location 50%, and fault resistance 100Ω

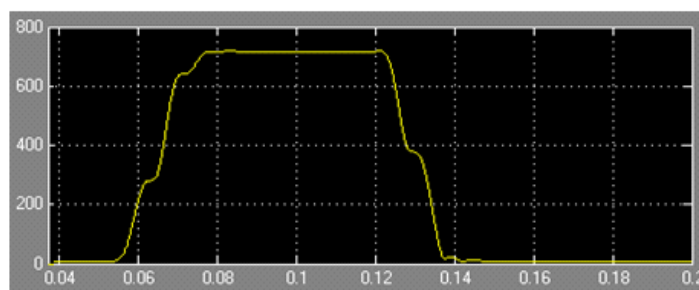


Fig. 11 Minimum positive sequence differential fault current 716A

Fig. 12 shows the Maximum differential fault current from the above fault analysis table for the condition L-L-L-G Fault, 90° inception angle, fault location 90%, and fault resistance 0.001Ω

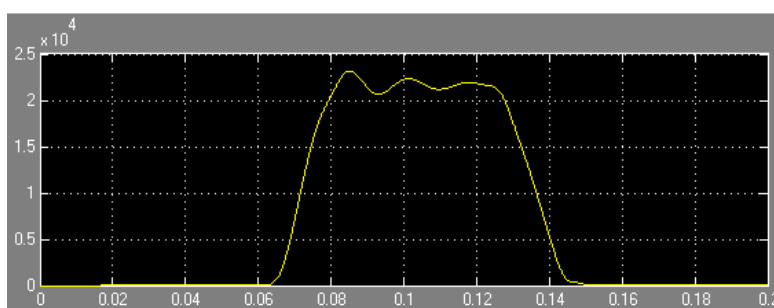


Fig. 12 Maximum positive sequence differential fault current 21.408KA

3.2.5 Conclusions From Table And Graphs

After studying all the types of faults under various conditions, we observe that minimum fault current occurs for L-G fault at 50% with high fault resistance (100Ω). The pick-up value of the relay should be set below this value, and above the value under normal condition.

IV. Conclusion

The results of the synchrophasors based current differential protection scheme shows that, whatever may be the type of fault, inception angle, fault resistance and fault location, the fault is being detected. Means this synchrophasors based current differential protection scheme gives almost 100% reliability, which would have not got in case of Distance protection scheme. Also, because of Global Positioning System (GPS) there is no limit on transmission line length which is to be protected. This feature of this technique makes it the better replacement for present Distance Protection system.

References

- [1]. Yuan R., Chen D., Yin X., Zhang Z., Ma T., Chen W.: 'Principle and property investigation of the transient current differential protection based on correlation analysis'. Presented at the IEEE Int. Conf. Power Engineering Society Winter Meeting, 2000, pp. 1945–1949
- [2]. Ito H., Shuto I., Ayakawa H., Beaumont P., Okuno K.: 'Development of an improved multifunction high speed operating current differential relay for transmission line protection'. Presented at the 7th IEE Int. Conf. Developments in Power System Protection, April 2001, pp. 511–514
- [3]. Z. Yining S. Jiale, "Phaselet-based current differential protection scheme based on transient Capacitive current compensation" IET Generation, Transmission, Distribution, 2008, Vol. 2, No. 4, pp. 469–477/469 doi: 10.1049/iet-gtd: 2007.0494.
- [4]. Jiale S., Xiaoning K., Guobing S., Zaibin J., Baoji Y.: 'Survey on relay protection using parameter identification', Proc. CSUEPSA, 2007, 19, (1), pp. 14–20
- [5]. Book: P. Kundur, "Power System Stability and Control", Tata McGraw-Hill Publication, 5th reprint 2008.
- [6]. Book: Sunil S. Rao, "Switch-Gear & Protection" Khanna Publishers, Delhi-6, 5th Edition